Nontrivial in-plane-magnetic-field dependence of THz wave emission from intrinsic Josephson junctions controlled by surface impedance

Yoshihiko Nonomura*
Computational Materials Science Center, National Institute for Materials Science, Tsukuba, Ibaraki 305-0047, Japan
(Dated: March 23, 2010)

Recently THz wave emission from intrinsic Josephson junctions (IJJs) was confirmed without external magnetic fields, and the surface impedance Z was found out to play a crucial role. When in-plane magnetic fields are introduced, field dependence of emission intensity also strongly depends on Z. For $Z = 1$, emission becomes the strongest when the wavelength of electromagnetic wave in IJJs coincides with the distance between Josephson vortices (JVs). For $Z \geq 3$, cavity resonance modes are stabilized and the fundamental mode gives the strongest emission. There occurs a dynamical phase transition between the π-phase-kink state (stable without external fields) and in-phase state as the in-plane magnetic field increases. Although the incommensurate-phase-kink state between these two states would be an artifact for small number of layers used in simulations, this artificial state almost vanishes for $Z \approx 50 \sim 60$, where field profile of emission intensity changes from a characteristic peak around 3/4 JVs per layer for smaller Z to monotonic decrease for larger Z. This crossover induced by Z may explain recent controversial experiments on the field profile of emission.

PACS numbers: 74.50.+r, 85.25.Cp, 74.25.Nf

Introduction. Although THz wave emission from intrinsic Josephson junctions (IJJs) had been investigated in in-plane external magnetic fields, experimental realization in such a condition [1] had been quite difficult. Recently evident THz wave emission was observed without external magnetic fields. [2, 3] In these experiments about a thousand of layers were included in IJJs so that the velocity of Josephson plasma mode is already as fast as that of light in IJJs, and only the fundamental ($n = 1$) cavity resonance mode has been observed so far. Then, possible emission states were investigated theoretically, and the uniform in-phase state [4, 5] and the π-phase-kink states with symmetry breaking along the c axis [6, 7] have been proposed. The present author showed [8] that these states are both stationary according to the bias current J and surface impedance Z, and drew the dynamical phase diagram in the Z-J plane. Quite recently emission in in-plane fields has been investigated again. In an experiment intensity decreases monotonically as the in-plane field increases, [9] while in another experiment the emission intensity seems to have some characteristic peaks in the field profile. [10] The present study suggests that these two experiments may not be controversial.

Model and formulation. As long as thermal fluctuations are not taken into account in the modeling, dimensional reduction along the in-plane magnetic field is justified. When the direction of the field is chosen as the y axis, the basic equations are given as follows, [11]

$$\partial_{x'}^2 \psi_{l+1,l} = (1-\zeta\Delta^{(2)}) \left(\partial_{t'} E'_{l+1,l} + \beta E'_{l+1,l} + \sin\psi_{l+1,l} - J' \right), \quad (1)$$

$$\partial_{t'} \psi_{l+1,l} = (1-\alpha\Delta^{(2)}) E'_{l+1,l}, \quad (2)$$

where the subscript "$l+1,l$" denotes quantities in the insulating layer between the l-th and $(l+1)$-th superconducting layers, and the operator $\Delta^{(2)}$ is defined in $\Delta^{(2)} X_{l+1,l} \equiv X_{l+2,l+1} - 2X_{l+1,l} + X_{l,l-1}$. Definitions of scaled quantities are given in Eqs. (7)–(10) of Ref. [8]. For example, length scale is scaled by the penetration depth in x', time scale by the inverse of plasma frequency in t', and bias current by the critical current in J'. In addition to the scaled electric field $E'_{l+1,l}$ and the gauge-invariant phase difference $\psi_{l+1,l}$, the scaled magnetic field is obtained from $\partial_{x'}\psi_{l+1,l} = (1-\zeta\Delta^{(2)}) B'_{l+1,l}$. Using the material parameters of $Bi_2Sr_2CaCu_2O_8$ given in Ref. [11], we have a large inductive coupling $\xi = 4.4 \times 10^5$ and a small capacitive coupling $\alpha = 0.1$, and $\beta = 0.02$ is taken.

Width of the junction $L_x = 86\mu$m is comparable to the size of samples in experiments, and for this size $B_y = 0.02$T corresponds to the condition "one JV per layer". Although a thousand of layer is essential for obtaining the plasma velocity as fast as that of light in IJJs, it is almost impossible to arrive at stationary states for such a large number of layers numerically at present. Then, the periodic boundary condition along the c axis is introduced instead. In such a condition plasma velocity of the stationary state automatically coincides with that of light in IJJs, though vanishing amplitude of electromagnetic waves on surfaces is totally neglected. Even if a thousand of layers are stacked, thickness of IJJ L_z is much smaller than the wavelength of emitted THz wave λ. In such a case emission is given by a point-like source (after two-dimensional reduction, by a line-like source in original three dimensions) and weaker than that from infinite sources. Such effect is approximately included as:

$$\partial_{x'}\psi_{l+1,l} = B'_{\rm ext} + \tilde{B}'_{l+1,l}, \quad (3)$$

$$\partial_{t'}\psi_{l+1,l} = \langle E'_{l+1,l} \rangle + \tilde{E}'_{l+1,l}, \quad (4)$$

$$\tilde{E}'_{l+1,l} = \mp Z \tilde{B}'_{l+1,l},\ Z = z\sqrt{\epsilon'_{\rm c}/\epsilon'_{\rm d}}, \quad (5)$$

with the dielectric constants of IJJs $\epsilon'_{\rm c}$ and dielectrics $\epsilon'_{\rm d}$,

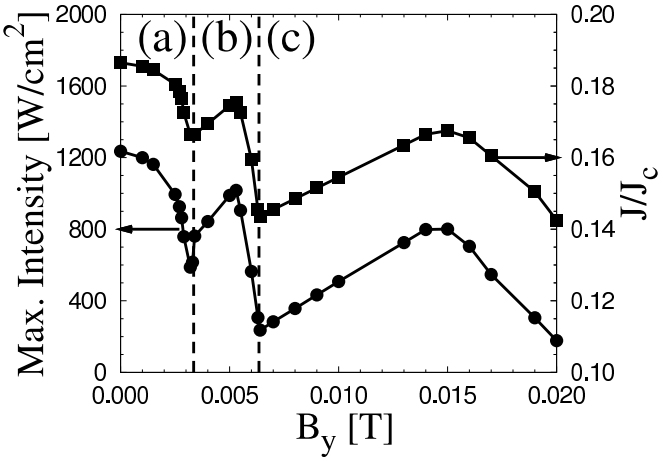

FIG. 1: Field dependence of maximum intensity in the $n = 1$ cavity resonance mode for $N = 4$ (circles) at the optimal bias current (squares). Dips of the curves stand for the dynamical phase transitions between the (a) π-phase-kink (π-PK), (b) incommensurate-phase-kink (IPK), and (c) in-phase states.

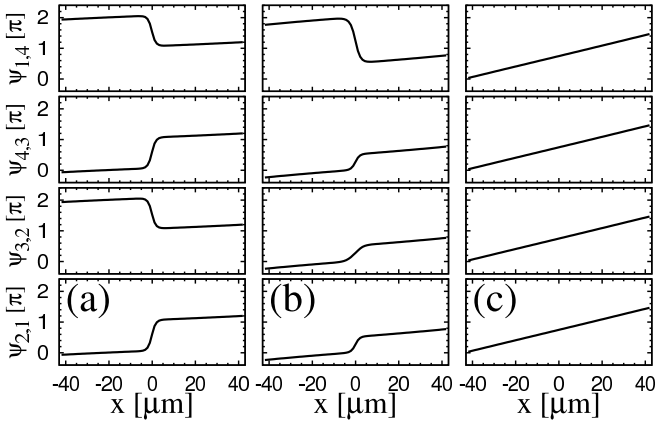

FIG. 2: Snapshots of gauge-invariant phase differences in all layers at (a) $B_y = 0.0033$T, $J = 0.166J_c$ (in the π-PK state near the phase boundary; two $\pm\pi$ kinks), (b) $B_y = 0.006$T, $J = 0.159J_c$ (in the IPK state near the phase boundary; three $+(1/2)\pi$ kinks and one $-(3/2)\pi$ kink), and (c) $B_y = 0.015$T, $J = 0.167J_c$ (in the in-phase state near the emission peak).

respectively. Here the dynamical parts of scaled boundary magnetic field $\tilde{B}'_{l+1,l}$ and electric field $\tilde{E}'_{l+1,l}$ are related with each other by $z \approx \lambda/L_z$. [12] Although this naive evaluation of z might be modified by excess magnetic fields from vertical directions omitted in two-dimensional modeling, [13] effect of impedance mismatch on the edges is also included in Z. Width of the sample L_x is divided into 80 numerical grids, and numerical calculations are based on the RADAU5 ODE solver. [14]

Numerical results for $Z = 1$. This condition is typically realized for $z = 1$ and $\epsilon'_c = \epsilon'_d$. Dependence of emission intensity on in-plane magnetic field and bias current was already investigated in Ref. [15]. Here the results are summarized for comparison with those for larger Z.

Aside from the recoupling region for small current, emission intensity takes the maximum value at the point where the wavelength of electromagnetic wave in IJJs and the distance between JVs coincide. From this condition and the ac Josephson relation, the current at the maximum intensity is proportional to the external magnetic field. The maximum intensity is independent of the current until it reaches the critical one J_c. On the contrary to previous numerical studies for $Z = 1$, [11, 16] no symptom of the cavity resonance remains in this simulation. In the previous studies number of layers is finite and effect of surface electrodes (penetration of superconductivity into electrodes) is taken into account, and this effect played a role of "cavity" even for $Z = 1$. Such an effect does not exist under the periodic boundary condition along the c axis. The frequency spectrum is quite sharp at the peak of emission intensity for each value of the in-plane magnetic field, and the frequency at emission peak is proportional to the in-plane magnetic field.

Numerical results for $Z = 10$. Similarly to the emission without external magnetic fields, the emission in the in-plane magnetic fields sharply depends on the value of the surface impedance Z. The cavity resonance modes are stable for $Z \geq 3$, and the fundamental ($n = 1$) mode becomes the strongest in in-plane magnetic fields. In the present article only the $n = 1$ mode is considered.

Field dependence of the maximum intensity with the optimal bias current for $Z = 10$ is shown in Fig. 1 by circles. Two dips in this figure divide the three dynamical states characterized by the structure of gauge-invariant phase difference shown in Fig. 2: (a) the π-phase-kink (π-PK) state stable without external fields, (b) the Incommensurate-phase-kink (IPK) state in the intermediate field region, and (c) the in-phase state. Field dependence of the current deriving the maximum intensity (optimal current) is also plotted in Fig. 1 by squares. Its shape is quite similar to that of the maximum intensity, and this field profile will not be shown hereafter.

The π-PK state is expected to be stable even for larger number of layers because stability of this state has already been confirmed without magnetic fields. If the in-phase state is stable, its property is expected to be independent of the number of layers. Then, peculiar layer-number dependence of physical properties may be seen in the IPK state. Field dependence of the maximum intensity for $N = 4$, 6, 8 and 12 is displayed around this region in Fig. 3, and typical snapshots of the gauge-invariant phase difference are shown in Figs. 4(a), 4(b) and 4(c) for $N = 6$, 8 and 12, respectively. These examples suggest that the IPK state for $N(= \textit{even})$ layers is characterized by $\pm(1 + 2/N)\pi$- and $\mp(1 - 2/N)\pi$-phase kinks with numbers $(N/2-1)$ and $(N/2+1)$, respectively.

Layer-number dependence of the phase boundaries shown in Fig. 3 is not trivial. The boundaries are determined by two factors: stability of each state and dif-

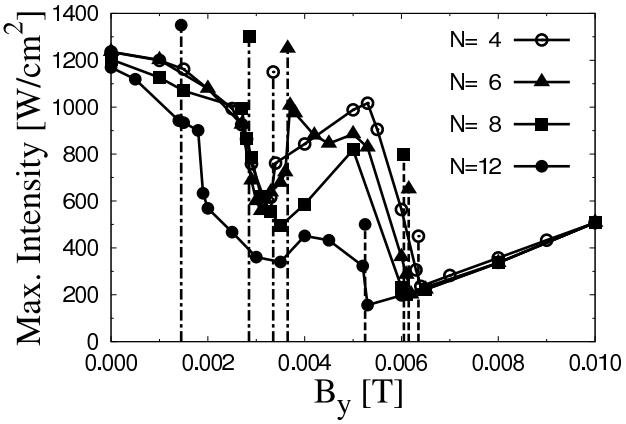

FIG. 3: Field dependence of maximum intensity in the $n = 1$ cavity resonance mode for $N = 4$ (open circles), 6 (full triangles), 8 (full squares), and 12 (full circles). Dash-dotted and dashed lines denote boundaries between the π-PK and IPK states and between the IPK and in-phase states, respectively.

ference between the states. The π-PK and in-phase states are well-defined independent of the number of layers N, while the IPK state varies as N does. Fig. 3 indicates that intensity of emission monotonically decreases as N increases in the IPK state, which suggests that this state becomes more and more unstable as N increases. It would be why the boundary between the IPK and in-phase states shifts to lower magnetic fields for increasing N. The boundary between the π-PK and IPK states is more nontrivial because similarity between the π-PK and IPK states also becomes stronger as N increases, and finally arrives at the same state in the $N \to \infty$ limit.

Then, the boundary fields between the π-PK, IPK and in-phase states are plotted versus inverse of layer numbers in Fig. 4(d). Since the boundary field between the π-PK and IPK states is expected to converge to $B_y = 0$ in the $N \to \infty$ limit, layer-number dependence of physical quantities can be checked by this condition. Fig. 4(d) shows that the naive $1/N$ plot is not bad (dash-dotted line versus full circles corresponding to the data for $N = 6$, 8 and 12). When the data for the boundary between the IPK and in-phase states (denoted by open circles) are extrapolated to $N \to \infty$ assuming similar N dependence (dashed lines), they clearly converge to a finite value. In summary, when the small-size effect of layer numbers is removed, there occurs one dynamical phase transition between the π-PK and in-phase states, and in this π-PK state the alternate arrangement of the $+\pi$- and $-\pi$-phase kinks [7] would be observed only in the vicinity of zero external field, and there would be a crossover to random arrangements of these two kinks.

Numerical results for other Z. As shown so far, emission behaviors for $Z = 1$ and 10 are quite different. This situation is similar to the zero-field case, and cavity-resonance properties become apparent for $Z \geq 3$. Field

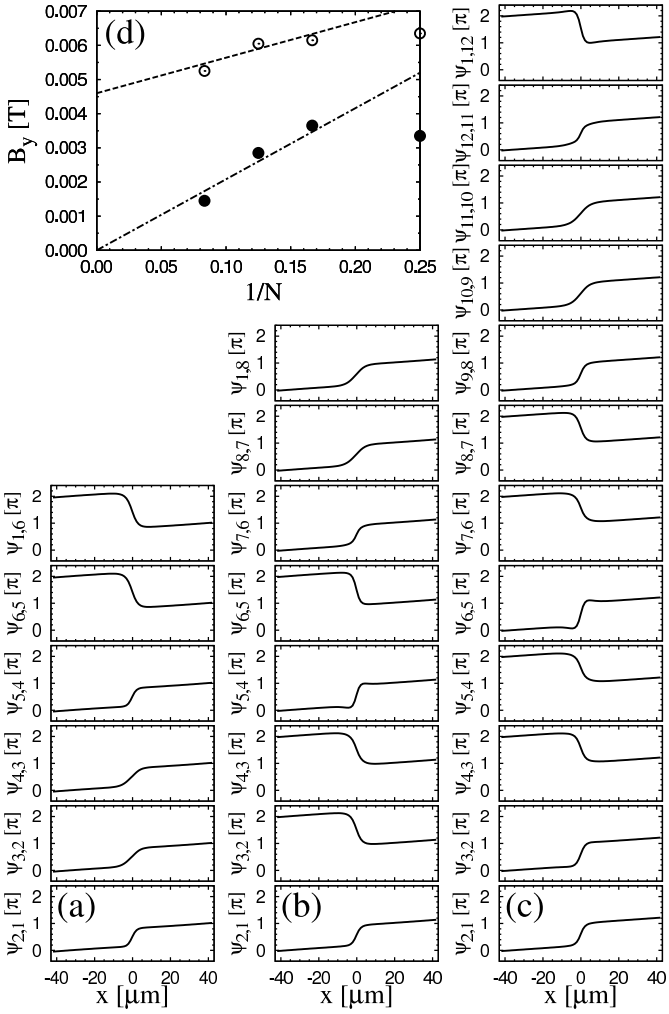

FIG. 4: Typical snapshots of gauge-invariant phase differences in all layers in the IPK region for (a) $N = 6$ (four $+(2/3)\pi$ kinks and two $-(4/3)\pi$ kinks), (b) $N = 8$ (five $+(3/4)\pi$ kinks and three $-(5/4)\pi$ kinks), and (c) $N = 12$ (seven $+(5/6)\pi$ kinks and five $-(7/6)\pi$ kinks). (d) Boundary fields between the π-PK and IPK states (full circles) and the IPK and in-phase states (open circles) versus inverse of layer number N. By naive linear extrapolation to the $N \to \infty$ limit, the former (dash-dotted lines) and the latter (dashed lines) seem to converge to $B_y = 0$ and a finite value of B_y, respectively.

dependence of maximum intensity of emission in this region of the $n = 1$ mode for $N = 4$ is given in Fig. 5(a) for $Z = 3$, 10, 30, 100 and 300 together with transition fields for each Z. This figure clearly indicates large Z dependence of the field profile of maximum intensity of emission. Although emission peak in the IPK region for $Z = 10$ and 30 is an artifact of small number of layers ($N = 4$), there is another emission peak in the in-phase state at $B_y \approx 0.015$T for $Z = 10$ and 30. On the other hand, there are no characteristic peaks for $Z = 100$ and 300; $B_y = 0.02$T (corresponding to 1 JV per layer) still belongs to the IPK region and even the field profile becomes almost field independent for $Z = 300$.

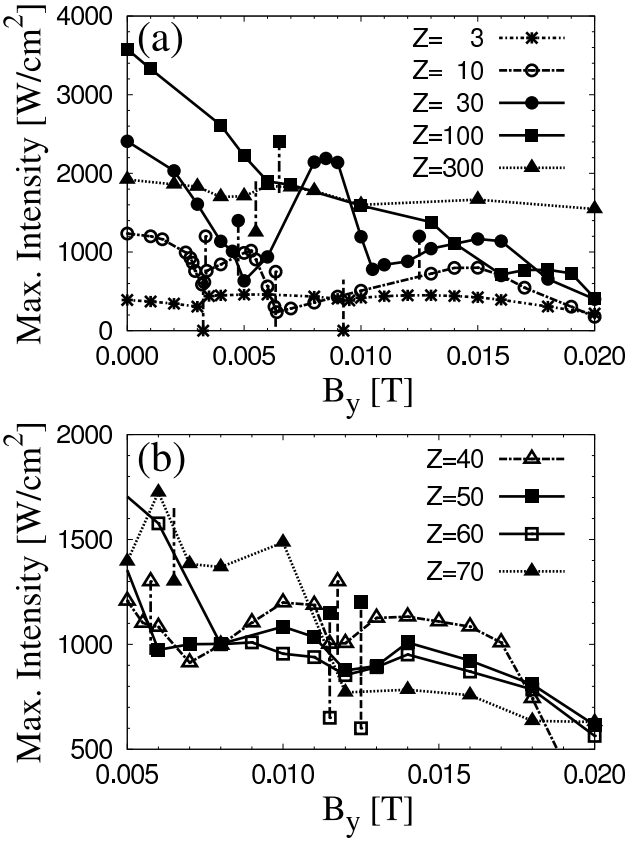

FIG. 5: Field dependence of maximum intensity for $N = 4$ for various values of the surface impedance Z: (a) for $Z = 3$ (stars), 10 (open circles), 30 (full circles), 100 (full squares) and 300 (full triangles), (b) expanded figure for $Z = 40$ (open triangles), 50 (full squares), 60 (open squares) and 70 (full triangles). In each figure dash-dotted and dashed lines denote boundaries between the π-PK and IPK states and between the IPK and in-phase states, respectively.

Then, Z dependence of the field profile of maximum intensity between $Z = 30$ and 100 is analyzed precisely. The field profile for $Z = 40$, 50, 60 and 70 is displayed in Fig. 5(b) together with transition fields for each Z. While the characteristic peak at $B_y \approx 0.015$T is still visible for $Z = 40$ as for $Z = 30$, it almost disappears for $Z = 50$ and 60, where the IPK region shrinks only around $B_y = 0.012$T. For $Z = 70$ the IPK region broadens and even $B_y = 0.02$T is included in this region as for $Z = 100$. That is, there exists a crossover between two different field profiles of maximum intensity at $Z \approx 50 \sim 60$.

Discussions. Quite recently there appear two experiments for THz wave emission from IJJs in in-plane fields based on the same samples for emission without magnetic fields. Welp *et al.* [9] observed monotonic decrease of emission intensity as the field increases, while Yamaki *et al.* [10] found characteristic peaks in the field profile of emission intensity. If such experimental conditions correspond to the crossover region at $Z \approx 50 \sim 60$, these two experiments may not be a serious controversy but a consequence of small difference in Z in the vicinity of the crossover point. This argument also suggests that values of Z in experiments may be much smaller than that naively expected from the relation $z \approx \lambda/L_z$ or $Z \approx 500$. It means that the argument by Tachiki *et al.* [13] that Z is effectively reduced by magnetic fields from vertical directions may be partially true, but that such effect is not so strong as they considered; they argued that Z may be reduced so much that the in-phase emission is observed.

Summary. THz wave emission from intrinsic Josephson junctions in in-plane magnetic fields is investigated numerically. Frequency-tunable emission by in-plane fields is observed for small surface impedance $Z < 3$, and cavity-resonant emission is observed for $Z \geq 3$. Experimentally-accessible $n = 1$ cavity resonance mode is the strongest, and there occur field-induced dynamical phase transitions between the π-phase-kink (π-PK), incommensurate-phase-kink (IPK) and in-phase states as the in-plane magnetic field increases. Investigation on size dependence of physical quantities on layer numbers N shows that IPK state may be an artifact of small N ($N \approx 1000$ in experiments) and that only the π-PK and in-phase states may be stable for large N. In the field profile of maximum intensity there exists a characteristic peak around 3/4 JVs per layer [10] for $Z \leq 40$, while it decreases monotonically [9] for $Z \geq 70$. This crossover of the field profile is characterized by sharp shrink of the IPK region even for $N = 4$ for $Z \approx 50 \sim 60$, which suggests that controversy of the field profile in recent experiments [9, 10] may be explained by slight difference in the surface impedance due to experimental conditions.

Acknowledgments. The present work was partially supported by Grant-in-Aids for Scientific Research (C) No. 20510121 from JSPS and by CREST program under JST.

* Electronic address: nonomura.yoshihiko@nims.go.jp

[1] M.-H. Bae *et al.*, Phys. Rev. Lett. **98**, 027002 (2007).
[2] L. Ozyuzer *et al.*, Science **318**, 1291 (2007); see also K. Lee *et al.*, Phys. Rev. B **61**, 3616 (2000).
[3] K. Kadowaki *et al.*, Physica C **468**, 634 (2008).
[4] H. Matsumoto *et al.*, Physica C **468**, 654, 1899 (2008).
[5] T. Koyama *et al.*, Phys. Rev. B **79**, 104522 (2009).
[6] S. Lin and X. Hu, Phys. Rev. Lett. **100**, 247006 (2008).
[7] A. E. Koshelev, Phys. Rev. B **78**, 174509 (2008).
[8] Y. Nonomura, Phys. Rev. B **80**, 140506(R) (2009).
[9] U. Welp *et al.*, on the APS March Meeting 2009, D34-1.
[10] K. Yamaki *et al.*, Physica C (2010), doi:10.1016/j.physc.2010.01.035.
[11] M. Tachiki *et al.*, Phys. Rev. B **71**, 134515 (2005).
[12] A. E. Koshelev and L. N. Bulaevskii, Phys. Rev. B **77**, 014530 (2008).
[13] M. Tachiki *et al.*, Phys. Rev. Lett. **102**, 127002 (2009).
[14] http://www.unige.ch/~hairer/software.html
[15] Y. Nonomura, J. Phys.: Conf. Ser. **150**, 052191 (2009).
[16] S. Lin *et al.*, Phys. Rev. B **77**, 014507 (2008).